



HAL
open science

Innovative machine learning approaches for nondestructive evaluation of materials

Roberto Miorelli, Christophe Reboud, Marco Salucci

► **To cite this version:**

Roberto Miorelli, Christophe Reboud, Marco Salucci. Innovative machine learning approaches for nondestructive evaluation of materials. EuCAP 2019 - 13th European Conference on Antennas and Propagation, Mar 2019, Cracovie, Poland. cea-04555968

HAL Id: cea-04555968

<https://cea.hal.science/cea-04555968>

Submitted on 23 Apr 2024

HAL is a multi-disciplinary open access archive for the deposit and dissemination of scientific research documents, whether they are published or not. The documents may come from teaching and research institutions in France or abroad, or from public or private research centers.

L'archive ouverte pluridisciplinaire **HAL**, est destinée au dépôt et à la diffusion de documents scientifiques de niveau recherche, publiés ou non, émanant des établissements d'enseignement et de recherche français ou étrangers, des laboratoires publics ou privés.

Innovative Machine Learning Approaches for Nondestructive Evaluation of Materials

Roberto Miorelli¹, Christophe Rebound¹, and Marco Salucci²

¹ CEA LIST, Gif-sur-Yvette, France, roberto.miorelli@cea.fr

² ELEDIA Research Center (ELEDIA@UniTN - University of Trento), Trento, Italy, marco.salucci@unitn.it

Abstract—This paper deals with a machine learning framework dedicated to nondestructive testing applications, in view of flaws detection and characterization. A supervised learning strategy is used on a training set made of characteristic features, extracted from eddy current testing (ECT) and ultrasounds testing (UT) signals. The approach is first presented and the key role of the feature extraction by means of Partial Least Squares is highlighted. Then, the performance of the proposed data-fusion approach, in terms of both localization and characterization, is compared to that of similar approaches exploiting one inspection technique only.

Index Terms—non-destructive testing and evaluation, data fusion, machine learning, eddy current testing, ultrasounds testing.

I. INTRODUCTION

In the context of non-destructive evaluation (NDE), there is an increasing need for fast and reliable tools in view of automatic flaw(s) detection, localization and characterization. Machine learning (ML) algorithms have shown to be suitable candidates for such tasks [1]. In the framework of eddy current testing (ECT) inspections, recent contributions [2, 3] established the link between their performance and the training set generation, from the viewpoint of feature extraction and the training set sampling strategy. The inspection method itself, i.e., the physics employed to probe the specimen, brings limitations in the inversion performance. In case of electromagnetic-based NDE techniques, like ECT for instance, the penetration of electromagnetic fields within the probed specimen depends on both the excitation frequency applied to the source and the medium electrical conductivity magnetic permeability. For this reason, ECT is widely employed in order to test conductive media (e.g., metal alloys) affected by surface or near to the surface cracks. Despite this, ECT present some advantages as it does not require any coupling material between the probe and the inspected specimen, is very reproducible and can be used at high speed. It is thus largely used in many industrial sectors like energy, manufacturing, metallurgy and aeronautic/aerospace. For the detection of cracks deeply buried under the piece surface, other inspection methods such as ultrasounds testing (UT) are preferred to ECT. In a ML paradigm, a fusion of information coming from both ECT and UT measurements can easily be carried out, through feature extraction. In this work, we implemented such fusion and evaluated its benefit versus that

of an algorithm employing a single-physic approach (i.e., ECT or UT).

The paper is structured as follows. In the next section, an introduction to the physical models employed to describe both interactions of electromagnetic field and ultrasounds pressure field with the specimen is provided. Subsequently, the ML paradigm adopted in this paper is outlined from the mathematical point of view. The numerical validation of the data fusion approach developed in this paper is discussed in Section III. Finally, conclusions and new research perspectives are drawn at the end of this paper.

II. MATHEMATICAL BACKGROUND

A. The forward model

The ECT physical solver employed in this work is based on the volume integral approach [4, 5] outlined hereafter. For sake of simplicity let us consider a homogeneous isotropic medium inspected by a coil working in absolute mode. The impedance variation due to a coil at a given position inspecting a conductive medium can be expressed via the reciprocity theorem [6] as

$$\Delta Z = \frac{1}{I^2} \int_V \bar{E}^{inc}(\vec{r}, \vec{r}') \cdot \bar{p}(\vec{r}, \vec{r}') dV, \quad (1)$$

where I stands for the current flowing through the coil spires, \bar{E}^{inc} represents the incident electric field and \bar{p} is the volume electric dipole density representing the secondary source due to the presence of a local inhomogeneity within the inspected medium. The vectors \vec{r}' and \vec{r} represent the source and the field points coordinates, respectively. The dipole density can be computed by solving numerically a Fredholm equation of the second kind, by means of the method of moments leading to the following system of equations

$$\left[\bar{E}^{tot} \right] = \left[\bar{E}^{inc} \right] - k^2 \left[\bar{G} \right] \left[\bar{p} \right]. \quad (2)$$

In (2), $\left[\bar{E}^{tot} \right]$ represents the discretized total electric field within the volume occupied by the flaw whereas $\left[\bar{E}^{inc} \right]$ is the incident field in the crack zone. $\left[\bar{G} \right]$ is the electric-electric dyadic Green function which is employed to express the effect of the electric dipole source $\left[\bar{p} \right]$ onto an electric field point laying within the discretized zone. k stands for the wave number associated to the medium where the flaw lies. In our numerical experiments, we have employed a hybrid UT model based on the physical theory of diffraction (PTD)

accounting Kirchhoff approximation (KA) and the physical theory of diffraction (GTD) [7]. According to [7], the scattered field by a defect embedded in a homogeneous medium can be described as

$$\begin{aligned} \bar{u}^{Scatt-PTD}(\bar{r}) = & \bar{u}^{Ray}(\bar{r}) + \bar{u}^{Kirc}(\bar{r}) + \sum_{\beta} \left(D_{\beta}^{\alpha GTD}(\bar{r}) - \right. \\ & \left. D_{\beta}^{\alpha KA}(\bar{r}) \right) \frac{e^{i l_{\beta} S_{\beta}}}{\sqrt{l_{\beta} S_{\beta}}} e_{\beta}(\bar{r}), \end{aligned} \quad (3)$$

where α is used to represent the longitudinal, transverse vertical or transverse horizontal incident waves and β the scattered waves counterparts. S_{β} is the distance between the diffraction point the observation point \bar{r} . $D_{\beta}^{\alpha GTD}(\bar{r})$ and $D_{\beta}^{\alpha KA}(\bar{r})$ represent the GTD and the Kirchhoff diffraction coefficients, respectively. Still in (3), \bar{u}^{Ray} and \bar{u}^{Kirc} are the displacement scatter field and the Rayleigh field, respectively. In this work, the obtained time-domain signals have been post processed in order to extract the peak value of the signal for each probe position considered within the scan.

B. The machine learning inverse model

A supervised machine learning framework has been employed in order to localize and characterize cracks. We first extract characteristics from both ECT and UT signals with the partial least squares (PLS) algorithm [8]. Then, an adaptive sampling strategy based on output space filling (OSF) algorithm [2] is performed in the PLS extracted feature space in order to collect the N samples representative of the final training set. We refer to this training set generation strategy as PLS-OSF in the following. The PLS-OSF approach has been adapted to a multi-physics context in which both the ECT extracted feature space and the UT extracted feature space should be sampled in parallel. This methodology can be summarized as follows:

1. **Initialization:** we initialize the training set by employing a tensor grid made by N_0 samples thus the forward solver for the ECT and the UT is evaluated on all the N_0 samples. The ECT ($\bar{D}^{\overline{ECT}}$) and the UT ($\bar{D}^{\overline{UT}}$) signals are then concatenated in order to obtain the initial training set $\bar{D}^{\overline{ECT-UT}} = \{ \bar{D}_n^{\overline{ECT}}, \bar{D}_n^{\overline{UT}} ; n = 1, \dots, N_0 \}$.

2. **PLS feature extraction:** the set of original features having size $F = N_0 \times K$ with K the number of concatenated ECT plus UT features are projected into the extracted feature space having size equal to $N_0 \times J$ where J represents the feature dimension via PLS algorithm [9] by solving the linear equation (4)

$$\left(\bar{D}^{\overline{ECT-UT}} \right)^T = \bar{T} \times \bar{S} + \bar{Y}, \quad (4)$$

where \bar{S} is the matrix of loadings \bar{Y} contains the so-called residuals. \bar{T} is the matrix that contains the compressed information (i.e., the extracted feature) is found as $\left(\bar{D}^{\overline{ECT-UT}} \right)^T \times \bar{W}$ with \bar{W} is the so-called weight matrix, which has been calculated by employing SIMPLS algorithm [9].

3. **OSF adaptive sampling:** starting from the knowledge of \bar{W} , the most suitable sample to be added into the training set is chosen by projecting a set of new candidate points into the extracted and choosing the one that maximize its Euclidean distance with respect to the other samples already embedded within the training set. The adaptive sampling loop ends when the maximum number of training samples N is reached.
4. **Inverse ML model fitting:** once the training set generation phase is ended, an inverse ML model must be fit on the data. In this work, we fitted the training set data by employing the support vector machine regression (SVR) algorithm [10]. Other ML models can be considered at this stage such as neural network, kernel ridge regression, Gaussian process regression, etc. Nevertheless, we opted in favor of SVR since enables a the sparse representation of the solution along with the possibility to “attach” a statistical and a physics-grounded meaning to the SVR hyper-parameters that must be tuned in order to properly fit the data.

III. NUMERICAL VALIDATION

In this work, we addressed a test case involving the inspection of an aluminum 2024 plate having thickness equal to 6 mm, density equal to 2.77g/cm³ and conductivity equal to 18.7 MS/m. A through thickness hole having radius equal to 3.75 mm is implanted within the plate and different cracks departing radially from the hole with different configurations in terms of length, skew angle and depth have been considered (see Fig. 1). The inspection procedure consisted in probing a squared grid centered on the hole by collecting 81 by 41 equally spaced samples. The number of features associated to the raw signal was equal to 3321 and 6642 for UT and ECT method, respectively. That is, the fused raw signals consisted in 9963 features from which 20 extracted features have been retrieved via PLS algorithm. In order to enable predictions on a meaningful range of crack parameters, the initialization procedure has been done for crack length $l_c \in [3.0, 10.0]$ mm, crack ligament $\delta_c \in [0.0, 4.0]$ mm and crack skew angle $\theta_c \in [0.0, 90.0]$ deg. A full-tensor grid having 27 samples has been considered as initialization whereas the final number of samples added

with PLS-OSF algorithm was 216. In order to test the performance of the developed multi-physics

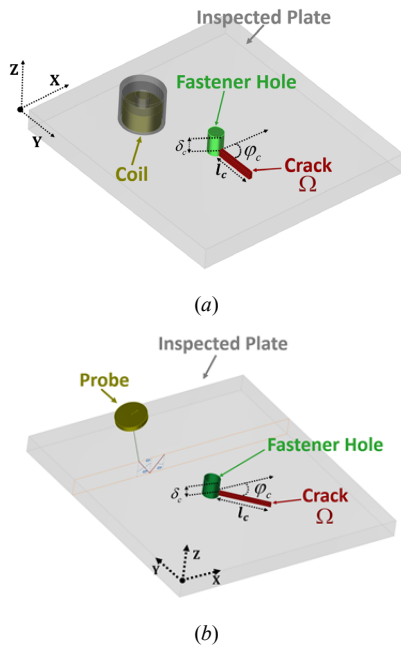


Fig. 1. Examples of studied (a) ECT and (b) UT configuration

strategy, we compare the former one with the respective single-physics counterparts (i.e., ECT or UT) on a synthetic test set composed of 1000 samples generated via a Latin hypercube sampling schema. Furthermore, the robustness of the proposed approach was assessed by considering the training set data blurred with additive white Gaussian noise (AWGN) having signal to noise ration equal to 10, 20, 30 and 40 dB.

In Fig. 2, we show the PLS-OSF sampling strategy results applied to ECT, UT and ECT-UT. One can notice that for all the three type of physics considered, the corresponding extracted feature space [i.e., Fig. 2 from (d) to (f)] result in an almost evenly sampled in contrast to the parameter space counterpart [i.e., Fig. 2 from (a) to (c)]. This is representative of the fact that the PLS-OSF algorithms tends to emphasize certain crack parameters for which the co-variance between data in the training set (i.e., the input parameters and the output signals) is maximized. From the physics point of view, these parameters are the ones that provide the strongest variation on the ECT and the UT signals collected by the probes. Furthermore, to these signals correspond the most critical crack configurations that one should be able to detect in the inversion procedure since are the most critical for possible integrity issues of the inspected medium.

Fig. 3 shows the prediction results obtained for the three physics in terms of normalized mean error (NME) [2] values considering the three crack parameters for different levels of AWGN corruption. We can notice that the data fusion approach (ECT-UT) yields the best results for all three

parameters retrieved, overcoming insufficiencies of each single-physics approach. From the computational point of view, the 1000 predictions shown in Fig. 3 has been obtained in about 0.03 seconds on a standard laptop, which means that almost real-time predictions are possible by employing the SVR inverse model developed in this paper.

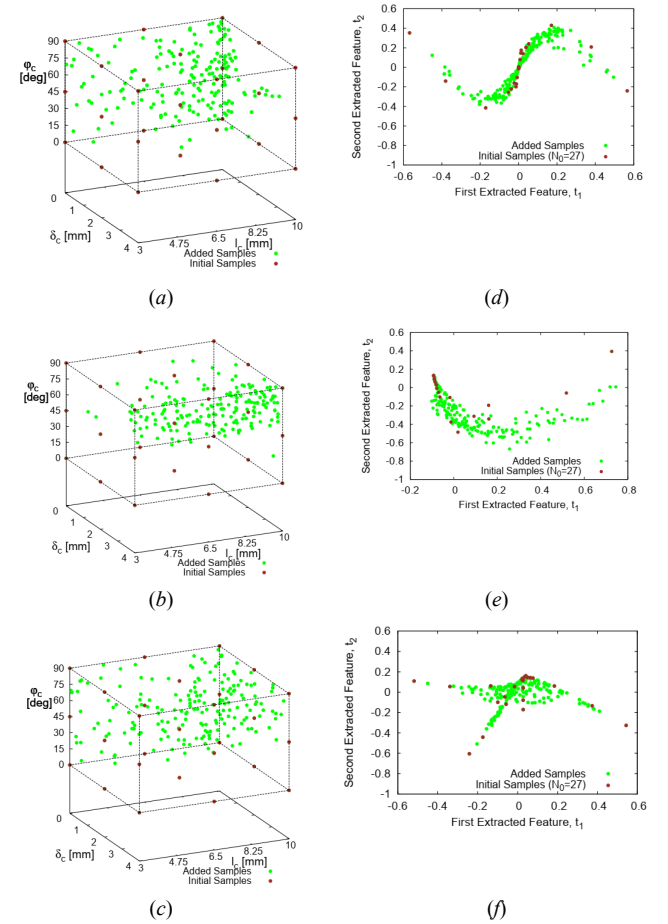


Fig. 2. Training samples mapped on (a)-(c) the crack parameter space, (d)-(f) the extracted feature space for (a)-(d) ECT, (b)-(e) UT and (c)-(f) ECT-UT while $N_0 = 27$, $J = 2$, $N = 216$.

IV. CONCLUSION AND PERSPECTIVES

This paper addresses a preliminary study of a multi-physics approach applied to NDT-NDE configuration in view of flaw(s) localization and characterization. We show that the proposed data fusion approach based on both ECT and UT improves the results of single physics separately when the PLS-OSF sampling strategy is performed in conjunction with a regression model based on SVR. The methodology developed in this paper can be straightforwardly applied to other multi-physics approaches in the NDT framework, such as the coupling between ECT and infrared thermography testing for instance. Moreover, time domain UT raw signal could be also considered in the future to increase the performance from the accuracy point of. As a last point, improvements of the proposed OSF-PLS sampling procedure can be done by frame the sampling

schema in a semi-supervised paradigm for which clustering, Gaussian mixture models, kernel density estimation etc. can be employed instead a metric based on the iterative calculation of distance between extracted features.

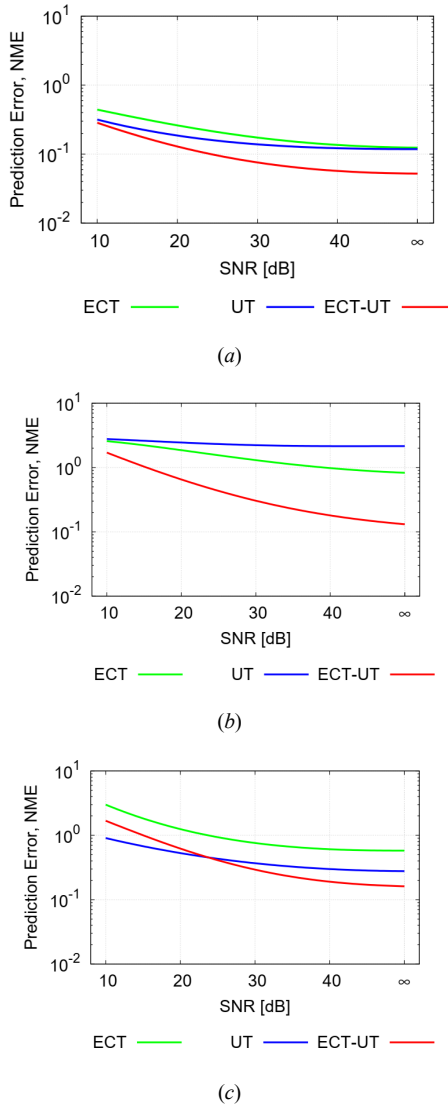


Fig. 3. NME vs. SNR representation for crack (a) length l_c , (b) ligament δc and (c) angular position θ_c estimation for $N = 216$, $J = 20$, $M = 1000$ through ECT, UT and ECT-UT data.

The outcomes of this approach consists in an higher efficiency in the training set generation phase (use of cluster calculation possible) and the possibility to treat very large signals such as time domain signals in UT, ground penetrating radar or x-ray tomography for instance.

REFERENCES

[1] A. Massa, G. Oliveri, M. Salucci, N. Anselmi, and P. Rocca, 'Learning-by-examples techniques as applied to electromagnetics', *Journal of Electromagnetic Waves and Applications*, vol. 32, no. 4, pp. 516–541, Mar. 2018.

[2] M. Salucci *et al.*, 'Real-Time NDT-NDE Through an Innovative Adaptive Partial Least Squares SVR Inversion Approach', *IEEE Transactions on Geoscience and Remote Sensing*, vol. 54, no. 11, pp. 6818–6832, Nov. 2016.

[3] M. Salucci, S. Ahmed, and A. Massa, 'An adaptive Learning-by-Examples strategy for efficient Eddy Current Testing of conductive structures', in *2016 10th European Conference on Antennas and Propagation (EuCAP)*, 2016, pp. 1–4.

[4] D. Lesselier and A. Razek, 'Eddy current scattering and inverse scattering, Green's integral and variational formulations.', in *Scattering and Inverse Scattering in Pure and Applied Science: Part 1 – Scattering of Waves by Macroscopic Targets*, E. Pike and P. C. Sabatier, Eds. Academic Press, 2002, pp. 486–507.

[5] R. Miorelli, C. Reboud, T. Theodoulidis, N. Poulakis, and D. Lesselier, 'Efficient modeling of ECT signals for realistic cracks in layered half-space', *IEEE Transactions on Magnetics*, vol. 49, no. 6, pp. 2886–2892, Jun. 2013.

[6] B. A. Auld, 'Eddy Current Characterization of Materials and Structures,' ASTM STP 722, edited by G. Birnbaum and G. Free (American Society for Testing and Materials, Philadelphia, 1981)

[7] V. Zernov, L. Fradkin, and M. Darmon, 'A refinement of the Kirchhoff approximation to the scattered elastic fields', *Ultrasonics*, vol. 52, no. 7, pp. 830–835, Sep. 2012.

[8] S. Wold, M. Sjöström, and L. Eriksson, 'PLS-regression: a basic tool of chemometrics', *Chemometrics and Intelligent Laboratory Systems*, vol. 58, no. 2, pp. 109–130, Oct. 2001.

[9] S. de Jong, 'SIMPLS: An alternative approach to partial least squares regression', *Chemometrics and Intelligent Laboratory Systems*, vol. 18, no. 3, pp. 251–263, Mar. 1993.

[10] C.-C. Chang and C.-J. Lin, 'LIBSVM: A Library for Support Vector Machines', *ACM Trans. Intell. Syst. Technol.*, vol. 2, no. 3, pp. 27:1–27:27, May 2011.